Discovery of Inter-Domain Stabilizers—A Novel Assay System for Allosteric Akt Inhibitors

ARTICLE *in* ACS CHEMICAL BIOLOGY · JUNE 2014

Impact Factor: 5.33 · DOI: 10.1021/cb500355c · Source: PubMed

8 AUTHORS, INCLUDING:

Zhizhou Fang
AbbVie
8 PUBLICATIONS **78** CITATIONS
SEE PROFILE

Dennis Plenker
University of Cologne
7 PUBLICATIONS **309** CITATIONS
SEE PROFILE

Hoang Duc Nguyen
VNUHCM-University of Science, Vietnam
28 PUBLICATIONS **505** CITATIONS
SEE PROFILE

Trang Thi Phuong Phan
Ho Chi Minh City University of Science
17 PUBLICATIONS **182** CITATIONS
SEE PROFILE

Discovery of Inter-Domain Stabilizers - A Novel Assay System for Allosteric Akt Inhibitors

Zhizhou Fang[1,2], Jeffrey R. Simard[2], Dennis Plenker[3], Hoang D. Nguyen[2], Trang Phan[2], Patrik Wolle[1], Stefan Baumeister[1], Daniel Rauh[1,2]*

[1] Technische Universität Dortmund, Fakultät für Chemie und Chemische Biologie, Otto-Hahn-Strasse 6, 44227 Dortmund, Germany.

[2] Chemical Genomics Centre of the Max Planck Society, Otto-Hahn-Strasse 15, 44227 Dortmund, Germany.

[3] University of Cologne, Department of Translational Genomics, Weyertal 115b, 50931 Cologne, Germany.

* To whom correspondence should be addressed.

Phone: +49 (0)231 - 755 7080. Fax: +49 (0)231 - 755 7082.

Email: daniel.rauh@tu-dortmund.de

Abstract

In addition to the catalytically active kinase domain, most kinases feature regulatory domains that govern their activity. Modulating and interfering with these inter-domain interactions presents a major opportunity for understanding biological systems and developing novel therapeutics. Therefore, small molecule inhibitors that target these interactions through an allosteric mode of action have high intrinsic selectivity, as these interactions are often unique to a single kinase or kinase family. Here we report the development of iFLiK (interface-FLiK), a fluorescence-based assay that can monitor such inter-domain interactions. Using iFLiK, we have demonstrated selective detection of allosteric Akt inhibitors that induce an inactive closed conformation unique to Akt. This methodology easily distinguished small molecule allosteric inhibitors from classic ATP-competitive inhibitors. Screening an in-house compound library with iFLiK, we were able to identify novel compounds with a scaffold that has not been previously described for allosteric Akt inhibitors.

Two decades of extensive kinase research have provided a substantial number of kinase inhibitors of various types[1,2]. The compounds have found great application as probes to dissect and understand kinase function in the context of signaling networks and as therapeutics for the treatment of diseases such as cancer, arthritis, autoimmune disorders, allergies or diabetes[3-8]. The majority of these inhibitors target the enzymatic activity of the kinase. However, recent studies clearly showed that kinase regulation extends beyond their capacity to phosphorylate other proteins[9]. In fact, it has been demonstrated that kinases also serve as scaffolding proteins to form multi-enzyme complexes or by competing for and disrupting protein-protein interactions. Although many examples are known so far, even more functions remain unexplored as different kinase conformations allow for a variety of interactions with other binding partners. The challenge for the next decade will be to understand these underlying scaffolding relationships in more detail. Investigating these interactions will not only provide insight into the complex issue of yet unexplored cellular signaling networks. In addition, modulators of such interactions also have various advantages over the more classical competitive inhibitors with respect to the pharmacological perturbation of disease states, thereby providing new avenues for drug development. For example, MK-2206 (**4**), an allosteric inhibitor of Protein Kinase B (PKB, also known as Akt), is currently in phase II clinical trials for the treatment of various cancers. In comparison to ATP-competitive Akt inhibitors, which all previously failed clinically, MK-2206 exhibited superior selectivity, good pharmacodynamic properties, and was well tolerated in clinical studies[10]. These favorable characteristics are owed to its allosteric mode of action, whereby the drug occupies a unique pocket formed at the interface of the catalytically active kinase domain and the regulatory pleckstrin homology domain (PH domain), thereby locking the kinase in a closed conformation and preventing the adaptation of the active state (**Fig. 1b**).

Some other small molecules are already known that modulate kinases *via* kinase-specific mechanisms, e.g. by stabilizing inactive conformations, preventing the formation of activated complexes or mimicking by native activators[11]. However, such discoveries are few in numbers and usually arise by chance. Therefore, there is an urgent need for methods that can identify novel compounds with such modulating functions. As these regulatory processes are likely to be associated with conformational changes in the complex architecture of intra- and intermolecular protein domain interactions, developing methods which enable the monitoring of protein-protein interactions and overall protein conformations can facilitate the identification of such modulators. In our group, we have previously developed the FLiK (Fluorescent Labels in Kinases) and FLiP (Fluorescent Labels in Phosphatases) high-throughput binding assays[12], which utilize solvatochromic fluorophores to report on conformational changes of various kinase structural elements that are part of the binding pocket, including the "MAPK insert", activation loop and glycine-rich loop of cSrc, p38α and *Um*GSK3[13-17], and the αI-helix of Abl[18]. Herein, we describe the development of the novel iFLiK technology (interface-FLiK) that can detect more complex changes in protein kinase conformations as well as intramolecular inter-domain interactions. We also describe its application in selectively identifying allosteric inhibitors of Akt.

RESULTS

Assay Design & Development

The protein kinase Akt plays a pivotal role in signaling pathways responsible for cell survival, proliferation and apoptosis[19]. Hyperactive Akt signaling has been shown to override apoptosis, thereby supporting increased proliferation of misregulated cells which, most importantly, renders these cells resistant to treatment by chemo- and radiotherapy[20]. Inhibition

of Akt has been shown to restore sensitivity towards apoptotic signaling and decrease tumor size in patients.

In addition to its kinase domain, Akt is allosterically regulated by phosphatidylinositol lipids which bind to the adjoined PH domain of Akt and trigger its recruitment to the plasma membrane[21]. In the inactive conformation ("PH-in" or "closed"), the PH domain moves in and forms tight interactions with the kinase domain *via* polar contacts and, in doing so, buries access to the ATP binding pocket. Upon upstream signaling by external growth factors and PI3K, phosphatidylinositol (3,4,5)-trisphosphate (PIP_3) binds to the PH domain of Akt, inducing the dissociation of the two domains from each other[22]. In this "open" (or "PH-out") conformation, Thr308 on the activation loop and Ser473 at the C-terminus of Akt can be phosphorylated by the kinases PDK1 and PDK2, respectively, to activate Akt[23].

In 2005, Lindsley *et al.* reported the serendipitous discovery of Akt inhibitors that only inhibited the full-length kinase but not the kinase domain alone (ΔPH)[24]. While these compounds were discovered by chance and their mode of action was initially unknown, these allosteric inhibitors proved to exhibit superior selectivity by addressing the unique activation mechanism of Akt. This discovery spawned the synthesis of a large library of diphenylquinoxalines and derivatives thereof (**Fig. 1a**)[25,26]. Further drug development resulted in the clinical candidate MK-2206, which is currently in phase II clinical trials[10]. The first crystal structure of the full-length Akt by Wu *et al.* (PDB entry 3O96) revealed that these inhibitors bind at the interface of the PH and kinase domain, locking them in the "closed" conformation[27]. The ATP pocket is then both inaccessible and disordered, preventing ATP and other substrates from binding.

Given the great promise of allosteric kinase inhibitors, there is an unmet need for novel assay systems that can specifically detect compounds with such a unique mode of action. Therefore, we sought to develop an assay system that allowed for the identification of

molecules that target Akt and stabilizes the enzyme in a catalytically inactive conformation (**Fig. 1c**). In order to achieve the highest possible sensitivity, a reporter fluorophore which is sensitive to the local charge environment of proteins must be introduced close to the domain interface without disrupting inter-domain interactions. At the time, no crystal structure of the full-length Akt had been published. After analyzing the calculations and mutagenesis studies by Calleja *et al.* on the interaction between the PH and kinase domain of Akt, we proposed Glu49 as a suitable labeling position[28] (**Supplementary Video 1**). The subsequently published X-ray crystal structures (PDB entries 3O96 and 4EJN) confirmed that Glu49 is sufficiently close to the domain interface[29]. For the selective labeling of the thiol-reactive reporter fluorophore at the desired position, we introduced the mutation Glu49Cys into Akt1 and removed all surface-exposed cysteines by convertion into serine residues (Cys296Ser, Cys310Ser, Cys344Ser). This construct was introduced into a baculovirus system for expression in stably transfected TriEx Sf9 cells. Purification with nickel affinity and size exclusion chromatography yielded the purified protein, which was subsequently labeled with the reporter fluorophore. Tryptic digests with subsequent MS/MS analysis confirmed the successful and selective labeling at Cys49 (**Supplementary Fig. 7**).

Since there were only a limited number of commercially available allosteric inhibitors to use as probes to validate our binding assay, we synthesized a focused library of MK-2206-type inhibitors (**7a-g**; **Fig. 2c**). Selectivity in *in vitro* and cellular activity tests (**Fig. 2d**) confirmed their allosteric mode of action. The detailed synthesis and results of the biological testing are described in the **Supplementary Information**. A collection of cysteine-reactive fluorophores (**Supplementary Fig. 3**) were used to label the purified protein and tested in combination with the clinical candidate MK-2206 as an allosteric reference inhibitor (positive detection control) and GSK690693 (**1**) as an ATP-competitive reference inhibitor (negative detection control). The fluorophores were excited at their respective excitation maxima, which

were determined in prior experiments. Depending on their structure, the various fluorophores displayed differential responses upon binding of the allosteric inhibitor (**Supplementary Fig. 4**). Some fluorophores like PyMPO or IANBD exhibited a shift in the emission spectrum and therefore in their fluorescence maximum, whereas an overall intensity increase could be observed with Atto565 or Eosin. Depending on the type of response observed, different assay readouts were used to determine ligand binding affinities. In the case of an intensity change, the fluorescence intensity at the emission maximum was used as the readout. In the case of spectrum shifting, the two wavelengths in the emission spectrum with half-maximal emission intensities were recorded, and the ratio of their emission intensities served as the assay readout. By comparing the fluorescence of the kinase incubated with 5 μM MK-2206 to the apo kinase (n = 6), signal-to-noise ratios and Z'-factors were calculated to characterize the assay quality and reproducibility for each Akt-fluorophore conjugate (Z' between 0.5 and 1 is generally considered ideal for high-throughput screening)[30]. All parameters and observed effects with the different reporter fluorophores are summarized in **Supplementary Table 2**. In addition, dose-response experiments were performed by incubating the labeled kinases with a dilution series of either MK-2206 or GSK690693 with final concentrations ranging between 0.8 nM and 50 μM. By plotting the respective assay response against the logarithmic inhibitor concentration, the K_d value was determined by fitting the data to a 4-point Hill function (**Supplementary Fig. 5**). Except for Atto 610 and acrylodan, all fluorophores were able to detect MK-2206 binding to Akt with comparable K_d values but with varying degrees of reliability. The response appeared to be specific for allosteric inhibitors since the labeled kinase was unresponsive to the addition of the ATP-competitive inhibitor GSK690693. In the case of Atto 610, no changes in the fluorescence spectrum could be observed with either inhibitor. For acrylodan, high levels of MK-2206 auto-fluorescence at the acrylodan excitation wavelength rendered the measurement with this reference inhibitor impossible. Therefore, experiments were repeated for acrylodan- and PyMPO-labeled Akt using the less

fluorescent **7b**, which revealed that acrylodan is also able to report on the conformational changes of Akt induced by allosteric inhibitors. For PyMPO, the assay response with **7b** was the same as with MK-2206. In summary, acrylodan and PyMPO proved to be the best performing probes for the iFLiK assay in terms of reliability. However, in order to avoid inhibitor auto-fluorescence, PyMPO was ultimately chosen for future experiments due to its excitation at longer wavelengths.

Following optimization of the assay, the allosteric Akt inhibitors MK-2206 and **7a-g** as well as the ATP-competitive inhibitors GSK690693 and CCT128930 (**2**) were tested with the PyMPO-labeled iFLiK construct in 384-well plates. Intrinsic compound auto-fluorescence was corrected by subtracting fluorescence intensities of the respective compounds, as measured alone in buffer. While the classic ATP-competitive Akt inhibitors had no effect on PyMPO fluorescence, the allosteric inhibitors provoked a bathochromic shift of the emission spectrum up to 16 nm, which allowed the determination of their K_d values (**Fig. 2a-b**). The SAR gained from the K_d values mirrored the IC_{50} values determined in the activity-based KinEASE assay, thereby validating the iFLiK approach. Mixtures of inhibitors with PyMPO-labeled glutathione or 2-mercaptoethanol, which carry comparably reactive thiol groups, displayed no such effect and confirmed that the observed responses were specific to the conformational change of Akt and not due to interactions with the fluorophores alone. As the binding pocket and iFLiK labeling site are more than 20 Å apart, an interaction between the ligand and the fluorophore (e.g. *via* resonance energy transfer or direct contact) is highly unlikely. Rather, the observation of fluorescence changes only when attached to Akt and not in the control studies confirmed that the observed spectral shifts were due to changes in the fluorophore environment induced by binding of the inhibitor to the allosteric site of the kinase. ATP-competitive inhibitors do not facilitate the closed conformation and, therefore,

were not detected by the iFLiK assay. This outcome successfully demonstrated the ability of iFLiK to report conformational changes of Akt induced by allosteric inhibitors.

To validate the assay results obtained with iFLiK using an independent measure of ligand binding, we employed the NanoTemper technology as an orthogonal assay, which measures changes in the diffusion kinetics of fluorophore-labeled proteins (in our case an amine-reactive Alexa Fluor 568) upon ligand binding in a temperature gradient due to microscale thermophoresis[31]. In order to assess the influence of PyMPO-labeling on Akt, two species (Akt labeled with AF568 only, and Akt labeled with AF568 and PyMPO) were measured independently with NanoTemper. For both species, K_d values determined using NanoTemper were comparable to the values obtained with iFLiK (**Supplementary Table 3** and **Supplementary Fig. 10**). The only exceptions were the weak inhibitors **7e** and **7g**, whose determined K_d values differed by about 2-4 fold. In contrast to iFLiK, NanoTemper was not able to distinguish between allosteric and ATP-competitive inhibitors since it detects all modes of binding, regardless of the binding conformation of Akt. Interestingly, binding affinities for the Alexa Fluor 568-labeled Akt did not differ significantly from the dually-labeled AF568-PyMPO protein. This suggests that PyMPO labeling of the Cys49 residue does not interfere with the inhibitor binding affinity. In contrast, mixtures of inhibitors with Alexa Fluor 568 alone (no kinase) displayed no thermophoretic effect. These findings confirm iFLiK as a valid assay technology to determine binding affinities for allosteric Akt inhibitors.

Screening of In-House Library

We screened our in-house library of over 10,000 compounds, consisting of both commercially purchased reagents as well as compounds synthesized in our laboratory for various projects. While fluorescence intensities were recorded at 508 nm (fl_{508}) and 638 nm (fl_{638}) to detect a shift of the emission spectrum, two different wavelengths (419 nm and 440 nm) were chosen for excitation of the fluorophore. To avoid intrinsic compound fluorescence, which is more

likely at shorter wavelengths, irradiation at 75% of the excitation maximum (440 nm in the case of PyMPO) was considered a good compromise to achieve maximum signal intensity and to minimize interference by auto-fluorescence. However, for compounds that produce fluorescence at 440 nm excitation are more likely to emit at 508 nm due to their smaller Stokes shift than PyMPO. In this case, excitation at 419 nm provided emission signals with less background fluorescence.

In this 1-point screen at 10 μM, the 24 compounds that displayed >25% binding relative to MK-2206 as 100% positive control were considered hits and selected for follow-up studies. Using dose-response measurements performed in triplicate, 13 out of 24 compounds were validated and produced a dose-dependent change in the fl_{508}/fl_{638} ratio (**Supplementary Fig. 11**). While the pyrrolo[2,3-*d*]pyrimidines **8a-c** evoked a bathochromic shift and **14** a hypsochromic shift in the PyMPO fluorescence spectrum, compounds like **15** also caused a reduction of the fluorescence intensity. In activity-based kinase assays (KinEASE by Cisbio), 12 of the 13 validated hits from the screen indeed inhibited Akt activity. However, the 9 compounds that reduced the PyMPO fluorescence in the iFLiK experiments showed inhibition of both full length Akt1 and ΔPH-Akt1. By contrast, the 3 compounds that solely provoked a bathochromic shift in the emission spectrum were selective for the full-length kinase, as would be expected for allosteric inhibitors.

In order to understand the observed SAR, binding modes of these compounds were calculated by docking these structures into published full length crystal structures of Akt (PDB codes 3O96 and 4EJN)[32], and two main binding modes were calculated by Glide from both crystal structures (**Fig. 3b**). To further understand the binding of these compounds, we obtained another 90 compounds based on this pyrrolopyrimidine scaffold from commercial sources and tested these to further explore the SAR (**Fig. 3a**). Structures of all 93 tested pyrrolopyrimidines are shown in **Supplementary Table 5**. The observed SAR is discussed in

more detail in the **Supplementary Information**. Seven of these 93 compounds **8a-g** responded in the iFLiK assay and exhibited selective inhibitory activity only on the full-length Akt1 as determined with the KinEASE assay. Upon treatment of the Akt-sensitive BT474 cell line with these seven pyrrolopyrimidines **8a-g**, a dose-dependent decrease in cell viability was observed with micromolar GI_{50}s (**Table 1**). Immunostaining of these BT474 cell lysates by Western Blot revealed a dose-dependent reduction in phosphorylation of the Akt substrate S6K, confirming Akt as the cellular target of **8a** and **8d** (**Supplementary Fig. 12**). With the profiling services of Life Technologies, **8a** and **8d** were profiled against a panel of 99 kinases (**Supplementary Table 6**) using an activity-based assay. Their activity profile show no effect on other kinases with PH domains or other members of the AGC kinase family, demonstrating their remarkable high inhibitory selectivity against Akt (**Supplementary Fig. 13**).

DISCUSSION

The highly dynamic conformational changes in proteins regulate their activity and binding affinity, including both intermolecular interactions with other molecules as well as intramolecular interactions with other protein domains. As Rauch *et al.* have demonstrated for kinases, these complex interactions (e.g. as scaffolding proteins) can effect intracellular localization and can have a far greater influence on their role in signaling networks than their catalytic function alone[9]. Investigations with the protein kinase Akt have shown that targeting such interactions can have a therapeutic value and can advance our understanding of biological systems. However, the discovery of a new species of small molecules capable of allosterically modulating such interactions has been hampered by the lack of suitable screening technologies. We aimed to address this issue with our novel iFLiK assay using the kinase Akt as a case study.

Akt labeling with the different fluorophores revealed that not all conjugates are equally suited to be probes for iFLiK. As expected, fluorophores with high dipole moments

were most sensitive to inhibitor binding since their Stokes shifts are more susceptible to polarity changes[33]. Previous in-house experiments showed that the emission spectra of acrylodan, PyMPO, IANBD and Texas Red were red-shifted (bathochromic) in solvents with increasing polarity, whereas DY-647 was blue-shifted (hypsochromic). Indeed, these shifts correlate with the observations in the assay, indicating a transition from a relatively nonpolar to a more polar environment upon inhibitor binding. This effect was observed for all fluorophores, suggesting a mechanism in which the reporter fluorophore is localized close to the protein surface, and is displaced by conformational reorganization of residues around the labeling site upon ligand binding, leading to an increased solvent exposure. Similar observations have been reported by Moreno *et al.* when investigating the effects of labeling human serum albumin with acrylodan[34]. Additionally, fluorophores with an internal rotor are known to exhibit increased fluorescence in environments of higher viscosity as the rate of rotational relaxation is reduced[35]. Therefore, an increased solvent exposure should lead to a reduced fluorescence quantum yield. In fact, a fluorescence increase was observed upon inhibitor binding to Akt labeled with Atto 565, Texas Red, Eosin and DY-647, suggesting a hindered fluorophore rotation due to close proximity to the protein surface. In comparison to Atto 565, the related fluorophore Atto 610 lacks the rotatable *para*-substituted phenyl moiety and hence does not display this emission increase. However, the magnitudes of these intensity changes were marginal and unreliable in most cases, and might be governed by factors other than rotational relaxation (e.g. rate of quenching). This result highlights the limitations of using fluorescence intensity at a single wavelength as a reliable assay readout instead of the preferred ratiometric readouts using emissions at two wavelengths.

In the singlicate high-throughput screen of 10,680 compounds, only 24 compounds showed a binding of >25% of the positive control at 10 μM, representing a hit rate of 0.22% (**Supplementary Fig. 10**). In the more detailed dose-response follow-up, 54% of the hits

identified for this cutoff could be validated, i.e. the overall false hit rate in this screen was 0.10% and the overall positive hit rate was 0.12%. Finally, of these validated hits, only one compound did not show an inhibitory effect in subsequent activity-based assays with Akt, demonstrating the high selectivity and reliability of the iFLiK binding assay. **8a-c** provoked a redshift of the PyMPO emission spectrum by up to 8 nm and inhibited the full-length Akt but not the truncated kinase, suggesting an allosteric mode of action that required the PH domain. On the other hand, the peptide derivative **14** produced a 5 nm blueshift, which would indicate a decrease of polarity in the environment surrounding the PyMPO sensor, an effect which was unique to this compound. In our working model for the assay, such a decrease of polarity around Cys49 could be interpreted as a shift in the equilibrium of the kinase toward the open conformation. Since this peptide shows Akt inhibition regardless of the PH domain presence, inhibition may occur *via* occupancy of the substrate pocket, which is only accessible in the open conformation. Such a binding mode would actually impede the association of the PH domain with the surface of the kinase domain. Interestingly, the sequence of **14** (CKKRRLKC) does not resemble any of the known peptide inhibitors of Akt[36-38]. However, the mode of action of this highly charged peptide will have to be further investigated in more detail. Compounds such as **15** also showed inhibition of both Akt1 and ΔPH-Akt1 and a slight redshift of 2 nm, but most prominently reduced the intensity of PyMPO fluorescence by up to 75%. Such hydrophobic, aromatic, poly-hydroxylic compounds are known to facilitate the non-specific aggregation and unfolding of proteins and regularly appear as hits in screening campaigns[39-41]. Therefore, the fluorescence decrease could be attributed to contact quenching by intermolecular collisions with proteins, due to a high local concentration of aggregates.

In the literature, some ATP-competitive Akt inhibitors with a pyrrolo[2,3-*d*]pyrimidine scaffold are known, such as the commercially available CCT128930[42]. However, these inhibitors form kinase hinge region contacts to Glu228 and Ala230 *via*

nitrogen atoms at the 1- and 7-positions of the chemical scaffold. An analogous binding mode is not possible for **8a-g** due to their bulky phenyl substituents. Instead, docking studies predicted two allosteric binding modes (**Fig. 3b**): Binding mode A resembles the conformation of **6** in 3O96, with the phenyl group at the 7-position exerting π-π-interactions with Trp80, and the phenyl group at the 5-position occupying the binding pocket of the **5** phenyl groups. In this position, the *N*1 atom of the pyrrolopyrimidine might replace the *N*5 atom of **5**, which is known to be crucial for inhibitory activity for these allosteric inhibitors[43]. Presumably, this nitrogen atom forms hydrogen bonds to Gln79, Thr81, Thr82, Asp292 and Gly294, mediated by a complex network of water molecules, that can be seen in the co-crystal structure of Akt1 with **6**. In addition, the thiophene group of **8a**, **8d**, **8e** and **8g**, as well as the pyridine group of **8b** and **8c** could take the place of the **5** piperidine group. In fact, this might explain the low efficacy of **8c** compared to **8b**, as the nitrogens in the *meta*-substituted pyridine of **8c** overlap better with the structure of **5** than those in the *ortho*-substituted **8b**. In binding mode B, the pyrrolopyrimidines are oriented like the original ligand **6** in the crystal structure 4EJN. Their *N*7 phenyl substituents expel the water molecules close to the protein surface, leading to a favorable entropic contribution to the Gibbs free energy of binding. In this conformation, the thiophene/pyridine/phenyl substituents and the phenyl group at the 5-position occupy the respective pyridine and phenyl positions of the original ligand. Furthermore, the exocyclic nitrogen atom at the 4-position might establish the aforementioned water network to the protein. In both binding modes, the lack of aromatic groups at the 4-position (as in **19f** or **21m**) would lead to a loss of affinity, as either one of the phenyl group pockets would no longer be occupied. However, binding mode A cannot explain the retained affinity of **8f**, as its phenyl group is unable to form the water-mediated hydrogen bond to Gln79. Binding mode B can explain the lack of effect of **8j** on Akt, since the thiophene group does not overlay with the pyridine group on **6** due to the presence of an additional methylene group of **8j**. However, neither of these binding modes can explain the dramatic decrease in

affinity upon introduction of a *meta* substituent at the *N*7 phenyl group, as in **8e** and **8g**. Follow-up synthesis of a more focused library of 4,5,7-substituted pyrrolo[2,3-d]pyrimidines will be required to explore their SAR in more detail.

The breast cancer cell line BT474, which is known to be sensitive to Akt inhibition by MK-2206-type inhibitors, showed a dose-dependent decrease in viability when incubated with **8a-g** and MK-2206[44]. In order to confirm the cellular target of these pyrrolopyrimidines, BT474 cells treated with increasing concentrations of MK-2206, **8a** and **8d** were further examined by immunostaining. While no significant reduction in phospho-Akt could be observed at concentrations up to 50 μM, which is consistent with the micromolar IC_{50}s in the biochemical assays (**Supplementary Fig. 11**), Akt inhibition could be detected by the reduction of the Akt substrate phospho-S6K, which is more sensitive towards Akt inhibition[45]. These findings further suggest that **8a-g** inhibit Akt activity.

In conclusion, we have developed a novel assay that can exclusively identify allosteric inhibitors of Akt by reporting on inter-domain conformational changes associated with the binding of such inhibitors. This class of allosteric inhibitors offers the possibility of selectively targeting single kinases or kinase families, allowing for a more precise dissection of kinase function and understanding of signaling pathways. Like most fluorescence-based assay technologies, iFLiK can be hampered by high intrinsic compound auto-fluorescence, depending on the applied fluorophore. However, this can be circumvented by choosing appropriate fluorophores as well as correcting for background fluorescence[46]. Mainly limited by the chemical space covered in compound libraries, this assay in particular allows the high-throughput screening for novel Akt inhibitors that stabilize the closed conformation of Akt. Since iFLiK is not an activity-based assay, it does neither require a prior activation of the kinase nor does it require a known substrate. Thus, iFLiK has two main advantages over activity-based assays: i) it enables the high-throughput search for novel chemical scaffolds

while the commercial screening of activated Akt with activity-based assays remains under patent protection and ii) allosteric MK-type inhibitors have a higher affinity toward the inactive kinase, allowing for the detection of weak binders that might otherwise be missed in activity-based assays. This increased sensitivity undoubtedly enabled the identification of **8a-c** as weak inhibitors. With iFLiK, we demonstrated an allosteric binding mode for **8a-g**, which was confirmed by the selective inhibition of full length Akt over the kinase domain alone in activity-based assays as well as inhibition of Akt activity in the Akt-sensitive BT474 cell line. Molecular modeling into the inter-domain binding pocket provided the means to understand the observed SAR of the measured compounds of this family. Such pyrrolopyrimidines have not previously been described in the literature as Akt inhibitors and will serve as the starting point for the synthesis of more focused compounds.

ACKNOWLEDGEMENTS

We thank Merck KGaA for their support with generating the baculovirus. We also thank Dr. Ralf Schneider for helpful discussions. This work was co-funded by the German federal state North Rhine Westphalia (NRW) and the European Union (European Regional Development Fund: Investing In Your Future) and the German Federal Ministry for Education and Research (NGFNPlus) (Grant No. BMBF 01GS08104).

AUTHOR CONTRIBUTIONS

Z.F. synthesized the compounds, developed the assay systems, determined K_d values with iFLiK and NanoTemper, and performed the docking experiments. J.R.S. and Z.F. designed the construct for labeling. D.P. conducted the BT-474 and H441 cell experiments. Z.F. expressed and purified the proteins with assistance from H.D.T. and T.P. IC_{50} values were determined by Z.F. and P.W. The synthesis protocols were further optimized by S.B. The

manuscript was prepared by Z.F. and D.R. with assistance by all co-authors. R.K.T. and D.R. designed the experiments.

METHODS

For detailed descriptions on synthetic protocols, construct design, protein expression, protein purification, fluorophore labeling, *in vitro* activity assays and cellular assays, see respective chapters in **Supplementary Methods**.

iFLiK Assay Development and Validation

Measurements were carried out in black 384-well plates (Greiner Bio One). Labeled Akt1 was diluted to 200 nM in the measurement buffer consisting of 50 mM HEPES pH 7.4, 200 mM NaCl and 0.01% Triton-X 100. Dilution series of candidate compounds were prepared in DMSO at 21X the final desired concentration. Compounds (0.5 µL) were then mixed with labeled Akt1 (10 µL) in triplicate and with measurement buffer alone (background fluorescence control) in quadruplicate at 12 different concentrations. The final compound concentrations ranged from 0.8 nM to 500 µM and each well contained 5% v/v DMSO after mixing. Plates were then covered with an adhesive plastic foil and incubated for 2 h at RT prior to measurement of emission intensities at fluorophore-specific wavelengths (**Supplementary Fig. 3**) using a Tecan Infinite M1000 plate reader. Compound auto-fluorescence was corrected for by subtraction of the average background signals obtained in the absence of labeled kinase. The respective assay readouts for the various Akt-fluorophore conjugates specified in **Supplementary Table 2** were fit to a Hill 4-parameter equation to determine K_d values for allosteric Akt ligands. Each reaction was performed in triplicate and at least three independent measurements of each K_d were determined for each ligand.

Screening with iFLiK

Screening initiatives were carried out in black 384-well plates (Greiner Bio One). PyMPO-labeled Akt1 was diluted to 200 nM in the measurement buffer consisting of 50 mM HEPES pH 7.4, 200 mM NaCl and 0.01% Triton-X 100. Each candidate compound was prepared in DMSO at 210 µM. Compounds (0.5 µL) were then mixed each with labeled Akt1 (10 µL) and with measurement buffer only to achieve final compound concentrations of 10 µM. Each well contained 5% v/v DMSO after mixing. Plates were then covered with an adhesive plastic foil and incubated for 2 h at RT prior to measurement of emission intensities at 508 nm and 638 nm using a Tecan Infinite M1000 plate reader, using both 419 nm and 440 nm for excitation. Compound auto-fluorescence was compensated by subtraction of the average background signals obtained in the absence of labeled kinase. Ratios of fluorescence intensities fl_{638}/fl_{508} were calculated from the background-subtracted values. For hit picking criteria, see **Supplementary Table 4**.

NanoTemper Assay Preparation & Execution

For the NanoTemper assay, 3 equivalents of Alexa Fluor 568 NHS ester were added to 50 µM kinase in a buffer consisting of 50 mM HEPES pH 8.3, 200 mM NaCl and 10% glycerol. After incubating 1 h in the dark at 4 °C, the protein was passed over a Superdex 75 10/300 GL (GE Healthcare) into a storage buffer consisting of 50 mM HEPES pH 7.3, 200 mM NaCl and 10% glycerol to remove unreacted fluorophore. The conjugated protein was then concentrated to approximately 30 µM, frozen in liquid nitrogen and stored at -80 °C.

Inhibitor dilution series at 21X of the final desired concentration were prepared in DMSO and then mixed with labeled Akt1 at 100 nM in a buffer consisting of 50 mM HEPES pH 7.4, 200 mM NaCl and 0.05% Tween-20. All solutions were incubated for 2 h at RT before transferring into enhanced gradient standard treated NanoTemper capillaries for measurement on a NanoTemper Monolith NT.115 using green excitation and emission filters. Capillaries

were illuminated at 25 °C with 90% LED power for 5 s. Thermophoresis was tracked for 45 s at 100% laser intensity, back-diffusion for 5 s. Fluorescence intensities were measured at 8-9 s and 49-50 s, and fluorescence intensity ratios of hot/cold were used as assay readout. K_d values were determined using the internal evaluation software.

FIGURES AND TABLES

Figure 1. Protein structure and schematic representation of iFLiK. a) Crystal structure of the full-length Akt protein. The PH domain (red) is tightly associated with the kinase domain (white), forming a binding pocket for Type IV allosteric inhibitors (orange spheres) at the domain interface, approximately 15 Å from the ATP binding pocket. A selection of known Akt inhibitors are shown. GSK690693 (**1**) and CCT128930 (**2**): commercially available ATP-competitive inhibitors. **3**: The first allosteric inter-domain inhibitor, found in a high-throughput campaign. MK-2206 (**4**): allosteric inhibitor currently in phase II clinical trials. Akti-1/2 (**5**): first allosteric inhibitor co-crystallized with full-length Akt (PDB code 3O96).[27] **6**: second allosteric inhibitor co-crystallized with full-length Akt (PDB code 4EJN).[29] b) Schematic representation of the Akt regulation mechanism. Akt exists in an equilibrium between an inactive conformation, in which the PH domain (red) binds to the kinase domain (white) and obstructs access to the ATP binding pocket, and an active open conformation. Inter-domain allosteric inhibitors (orange) bind into a hydrophobic pocket formed by residues of the PH domain – kinase domain interface, locking Akt in the closed, enzymatically inactive, conformation. c) Schematic assay principle: PH domain labeled covalently with reporter fluorophore *via* a synthetic cysteine (Glu49Cys). Transitions from open to closed conformations change the environment around the reporter fluorophore and therefore its fluorescence characteristics (blue and yellow spheres, respectively).

Figure 2. Fluorescent readout and results of the iFLiK assay. a) Allosteric inhibitors (MK-2206 shown here) cause a bathochromic shift of the PyMPO emission spectrum (maximum from 560 nm to 576 nm), whereas ATP-competitive inhibitors like GSK690693 show no effect. b) Using the ratio of fluorescence intensities at 638 nm and 508 nm as the assay readout, the emission shift can be quantified. Again, the ATP-competitive GSK690693 has no

effect. c) Structures of synthesized allosteric probe inhibitors **7a-g**. d) Testing of the biological effect of Akt inhibitors. *in vitro* IC_{50}s were determined with the KinEASE assay against full-length Akt1 and ΔPH-Akt1. Cellular GI_{50}s were determined with the CellTiter Glo assay against BT474 and H441 cell lines. K_ds were determined with the iFLiK assay. All values are expressed in μM. n.i. = not inhibiting up to 200 μM. n.e. = not effective up to 30 μM. n.r. = no response up to 500 μM. n.m. = not measured.

Figure 3. Novel allosteric Akt inhibitors with pyrrolopyrimidine scaffold identified in a high-throughput screen. a) Structures of compounds that showed an effect in activity and binding assays (**8a-g**) and a selection of inactive compounds (**8i-j**, **19f**, **21m**, **23d**). b) The two main binding modes for the pyrrolopyrimidines (**8a** shown as an example in purple sticks) as calculated by Glide. For reference in binding mode A (left) and B (right), the co-crystallized inhibitors **5** (orange sticks) from 3O96 and **6** (yellow sticks) from 4EJN are displayed, respectively. Asp292 of the kinase domain and Trp80 of the PH-domain are shown as sticks.

Table 1. Results of pyrrolopyrimidine inhibitors in binding (iFLiK) and activity (KinEASE) assays. n.i. = no inhibition up to 200 μM. n.r. = no response up to 500 μM.

	K_d	IC_{50} Akt1	IC_{50} ΔPH-Akt1	GI_{50} BT474
8a	2.2 ± 0.5 μM	196 ± 102 μM	n.i.	25 ± 8 μM
8b	7.8 ± 0.7 μM	160 ± 44 μM	n.i.	16 ± 5 μM
8c	20 ± 7 μM	n.i.	n.i.	49 ± 20 μM
8d	2.2 ± 0.7 μM	71 ± 30 μM	n.i.	13 ± 3 μM
8e	99 ± 61 μM	n.i.	n.i.	20 ± 6 μM
8f	6 ± 4 μM	>200 μM	n.i.	25 ± 5 μM
8g	264 ± 284 μM	>200 μM	n.i.	26 ± 5 μM
8i	n.r.	n.i.	n.i.	-
8j	n.r.	n.i.	n.i.	-
19f	n.r.	n.i.	n.i.	-
21m	n.r.	n.i.	n.i.	-
23d	n.r.	n.i.	n.i.	-

REFERENCES

1 Rabiller, M. *et al.* Proteus in the world of proteins: conformational changes in protein kinases. *Archiv der Pharmazie (Weinheim, Germany)* **343**, 193-206 (2010).

2 Cohen, P. & Alessi, D.R. Kinase drug discovery--what's next in the field? *ACS Chem. Biol.* **8**, 96-104 (2013).

3 Laplante, M. & Sabatini, D.M. mTOR signaling in growth control and disease. *Cell* **149**, 274-293 (2012).

4 O'Hare, T., Deininger, M.W.N., Eide, C.A., Clackson, T. & Druker, B.J. Targeting the BCR-ABL signaling pathway in therapy-resistant Philadelphia chromosome-positive leukemia. *Clin. Cancer. Res.* **17**, 212-221 (2011).

5 Cohen, P. Protein kinases--the major drug targets of the twenty-first century? *Nat. Rev. Drug Discov.* **1**, 309-315 (2002).

6 Hussain, K. *et al.* An activating mutation of AKT2 and human hypoglycemia. *Science* **334**, 474 (2011).

7 Racioppi, L. & Means, A.R. Calcium/calmodulin-dependent protein kinase kinase 2: roles in signaling and pathophysiology. *J. Biol. Chem.* **287**, 31658-31665 (2012).

8 Shaw, A.T. & Solomon, B. Targeting anaplastic lymphoma kinase in lung cancer. *Clin. Cancer. Res.* **17**, 2081-2086 (2011).

9 Rauch, J., Volinsky, N., Romano, D. & Kolch, W. The secret life of kinases: functions beyond catalysis. *Cell Commun. Signal.* **9**, 23 (2011).

10 Ma, B.B.Y. *et al.* Preclinical evaluation of the AKT inhibitor MK-2206 in nasopharyngeal carcinoma cell lines. *Investigational New Drugs* **31**, 567-575 (2012).

11 Fang, Z., Grütter, C. & Rauh, D. Strategies for the Selective Regulation of Kinases with Allosteric Modulators: Exploiting Exclusive Structural Features. *ACS Chem. Biol.* **8**, 58-70 (2013).

12 Schneider, R., Beumer, C., Simard, J.R., Grütter, C. & Rauh, D. Selective Detection of Allosteric Phosphatase Inhibitors. *J. Am. Chem. Soc.* **135**, 6838-6841 (2013).

13 Getlik, M. *et al.* Fluorophore labeled kinase detects ligands that bind within the MAPK insert of p38alpha kinase. *PLoS One* **7**, e39713 (2012).

14 Simard, J.R. *et al.* Fluorophore labeling of the glycine-rich loop as a method of identifying inhibitors that bind to active and inactive kinase conformations. *J. Am. Chem. Soc.* **132**, 4152-4160 (2010).

15 Simard, J.R. *et al.* High-throughput screening to identify inhibitors which stabilize inactive kinase conformations in p38alpha. *J. Am. Chem. Soc.* **131**, 18478-18488 (2009).

16 Simard, J.R. *et al.* Development of a fluorescent-tagged kinase assay system for the detection and characterization of allosteric kinase inhibitors. *J. Am. Chem. Soc.* **131**, 13286-13296 (2009).

17 Simard, J.R. *et al.* A new screening assay for allosteric inhibitors of cSrc. *Nat. Chem. Biol* **5**, 394-396 (2009).

18 Schneider, R. *et al.* Direct binding assay for the detection of type IV allosteric inhibitors of Abl. *J. Am. Chem. Soc.* **134**, 9138-9141 (2012).

19 Carnero, A. The PKB/AKT Pathway in Cancer. *Curr. Pharm. Des.* **16**, 34-44 (2010).

20 Falasca, M. PI3K/Akt Signalling Pathway Specific Inhibitors: A Novel Strategy to Sensitize Cancer Cells to Anti-Cancer Drugs. *Curr. Pharm. Des.* **16**, 1410-1416 (2010).

21 Barnett, S.F., Bilodeau, M.T. & Lindsley, C.W. The Akt/PKB Family of Protein Kinases: A Review of Small Molecule Inhibitors and Progress Towards Target Validation. *Curr. Top. Med. Chem.* **5**, 109-125 (2005).

22 Calleja, V., Laguerre, M. & Larijani, B. 3-D structure and dynamics of protein kinase B — new mechanism for the allosteric regulation of an AGC kinase. *Journal of Chemical Biology* **2**, 11-25 (2009).

23 Alessi, D.R. *et al.* Characterization of a 3-phosphoinositide-dependent protein kinase which phosphorylates and activates protein kinase Ba. *Curr. Biol.* **7**, 261-269 (1997).

24 Lindsley, C.W. *et al.* Allosteric Akt (PKB) inhibitors: discovery and SAR of isozyme selective inhibitors. *Bioorg. Med. Chem. Lett.* **15**, 761-764 (2005).

25 Barnett, S.F. *et al.* Identification and characterization of pleckstrin-homology-domaindependent and isoenzyme-specific Akt inhibitors. *Biochem. J* **385**, 399-408 (2005).

26 Siu, T. *et al.* The design and synthesis of potent and cell-active allosteric dual Akt 1 and 2 inhibitors devoid of hERG activity. *Bioorg. Med. Chem. Lett.* **18**, 4191-4194 (2008).

27 Wu, W.-I. *et al.* Crystal Structure of Human AKT1 with an Allosteric Inhibitor Reveals a New Mode of Kinase Inhibition. *PLoS One* **5**, e12913 (2010).

28 Calleja, V. *et al.* Intramolecular and Intermolecular Interactions of Protein Kinase B Define Its Activation In Vivo. *PLoS Biol.* **5**, 780-791 (2007).

29 Ashwell, M.A. *et al.* Discovery and Optimization of a Series of 3-(3-Phenyl-3H-imidazo[4,5-b]pyridin-2-yl)pyridin-2-amines: Orally Bioavailable, Selective, and Potent ATP-Independent Akt Inhibitors. *J. Med. Chem.* **55**, 5291–5310 (2012).

30 Zhang, J.-H., Chung, T.D.Y. & Oldenburg, K.R. A Simple Statistical Parameter for Use in Evaluation and Validation of High Throughput Screening Assays. *J. Biomol. Screen.* **4**, 67-73 (1999).

31 Wienken, C.J., Baaske, P., Rothbauer, U., Braun, D. & Duhr, S. Protein-binding assays in biological liquids using microscale thermophoresis. *Nature communications* **1**, 100 (2010).

32 Glide, version 5.6, Schrödinger, Inc., New York, NY, 2010.

33 Lippert, E. Spektroskopische Bestimmung des Dipolmomentes aromatischer Verbindungen im ersten angeregten Singulettzustand. *Z. Elektrochem.* **61**, 962-975 (1957).

34 Moreno, F., Cortijo, M. & González-Jiménez, J. Interaction of Acrylodan with Human Serum Albumin. A Fluorescence Spectroscopic Study. *Photochem. Photobiol.* **70**, 695-700 (1999).

35 Kuimova, M.K., Yahioglu, G., Levitt, J.A. & Suhling, K. Molecular Rotor Measures Viscosity of Live Cells via Fluorescence Lifetime Imaging. *J. Am. Chem. Soc.* **130**, 6672-6673 (2008).

36 Hiromura, M. *et al.* Inhibition of Akt Kinase Activity by a Peptide Spanning the A Strand of the Proto-oncogene TCL1. *J. Biol. Chem.* **279**, 53407-53418 (2004).

37 Cheng, J.Q., Lindsley, C.W., Cheng, G.Z., Yang, H. & Nicosia, S.V. The Akt/PKB pathway: molecular target for cancer drug discovery. *Oncogene* **24**, 7482-7492 (2005).

38 Tal-Gan, Y. *et al.* Backbone-Cyclic Peptide Inhibitors of Protein Kinase B (PKB/Akt). *J. Med. Chem.* **54**, 5154-5164 (2011).

39 McGovern, S.L., Caselli, E., Grigorieff, N. & Shoichet, B.K. A Common Mechanism Underlying Promiscuous Inhibitors from Virtual and High-Throughput Screening. *J. Med. Chem.* **45**, 1712-1722 (2002).

40 McGovern, S.L. & Shoichet, B.K. Kinase Inhibitors: Not Just for Kinases Anymore. *J. Med. Chem.* **46**, 1478-1483 (2003).

41 Coan, K.E.D., Maltby, D.A., Burlingame, A.L. & Shoichet, B.K. Promiscuous Aggregate-Based Inhibitors Promote Enzyme Unfolding. *J. Med. Chem.* **52**, 2067-2075 (2009).

42 Caldwell, J.J. *et al.* Identification of 4-(4-aminopiperidin-1-yl)-7H-pyrrolo[2,3-d]pyrimidines as selective inhibitors of protein kinase B through fragment elaboration. *J. Med. Chem.* **51**, 2147-2157 (2008).

43 Zhao, Z. *et al.* Discovery of 2,3,5-trisubstituted pyridine derivatives as potent Akt1 and Akt2 dual inhibitors. *Bioorg. Med. Chem. Lett.* **15**, 905-909 (2005).

44 She, Q.-B. *et al.* Breast Tumor Cells with PI3K Mutation or HER2 Amplification Are Selectively Addicted to Akt Signaling. *PLoS One* **3**, e3065 (2008).

45 Chandarlapaty, S. *et al.* AKT inhibition relieves feedback suppression of receptor tyrosine kinase expression and activity. *Cancer Cell* **19**, 58-71 (2011).

46 Schneider, R. *et al.* Overcoming compound fluorescence in the FLiK screening assay with red-shifted fluorophores. *J. Am. Chem. Soc.* **ASAP** (2013).

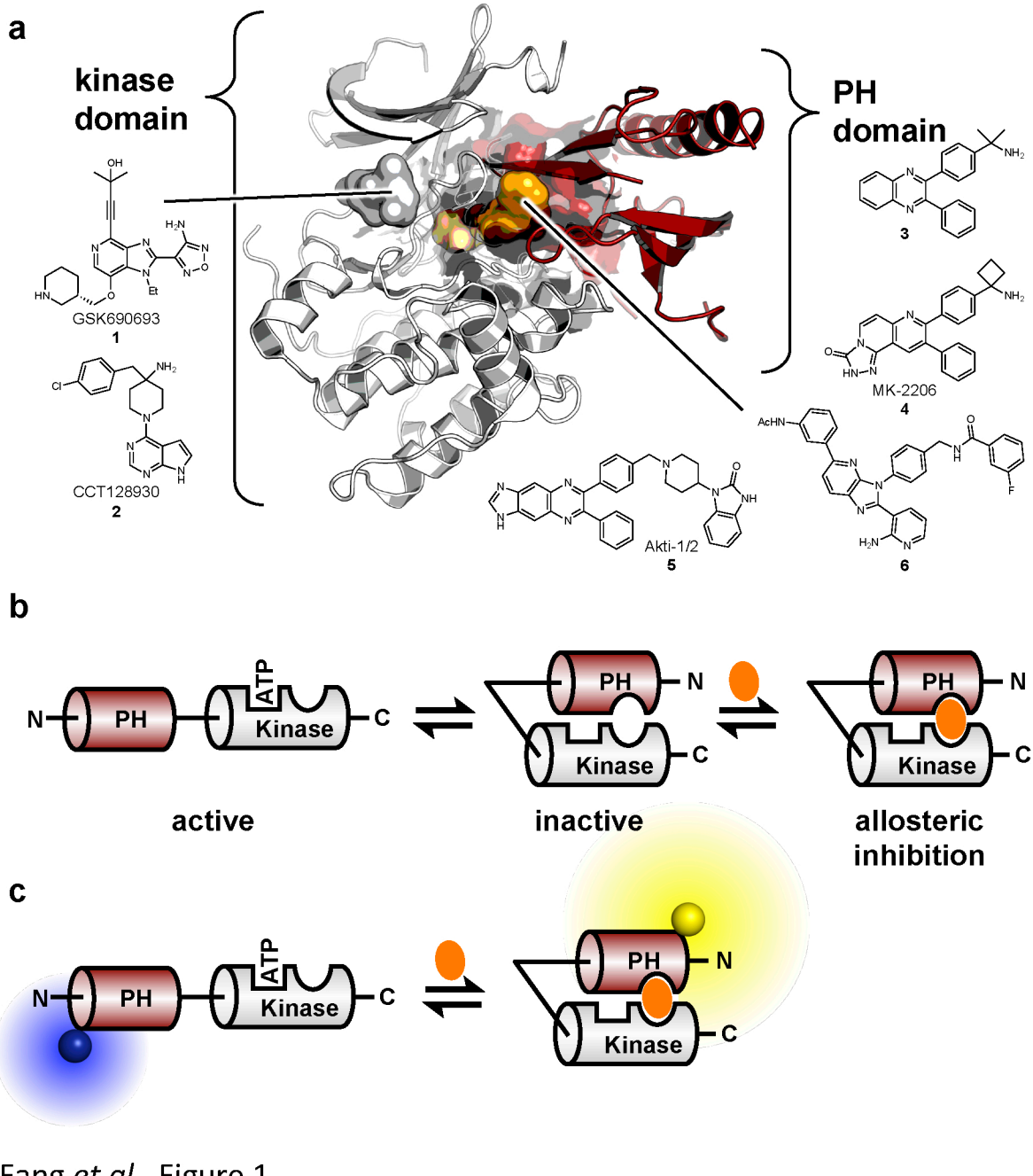

Fang *et al.*, Figure 1

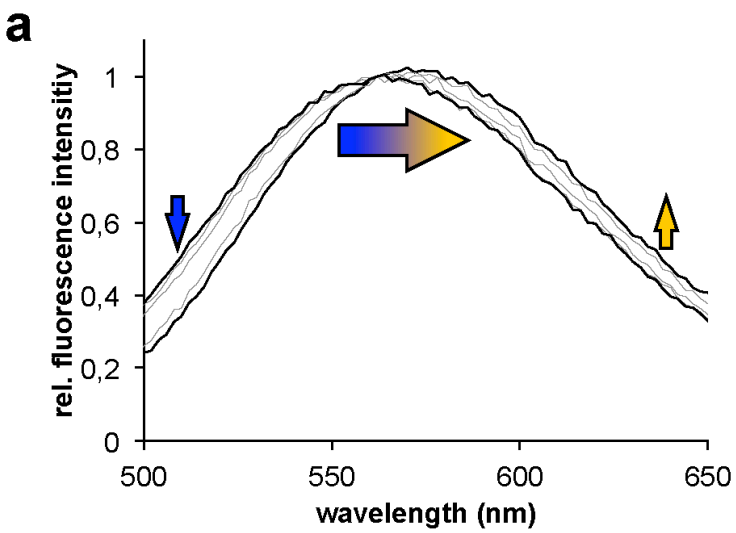

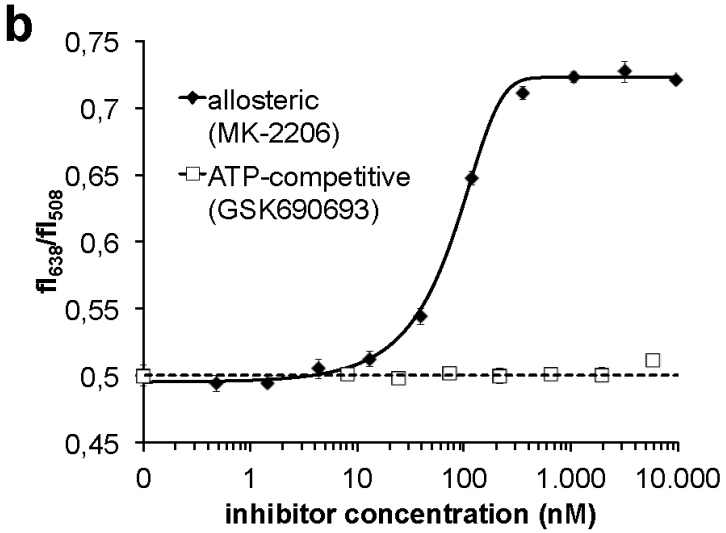

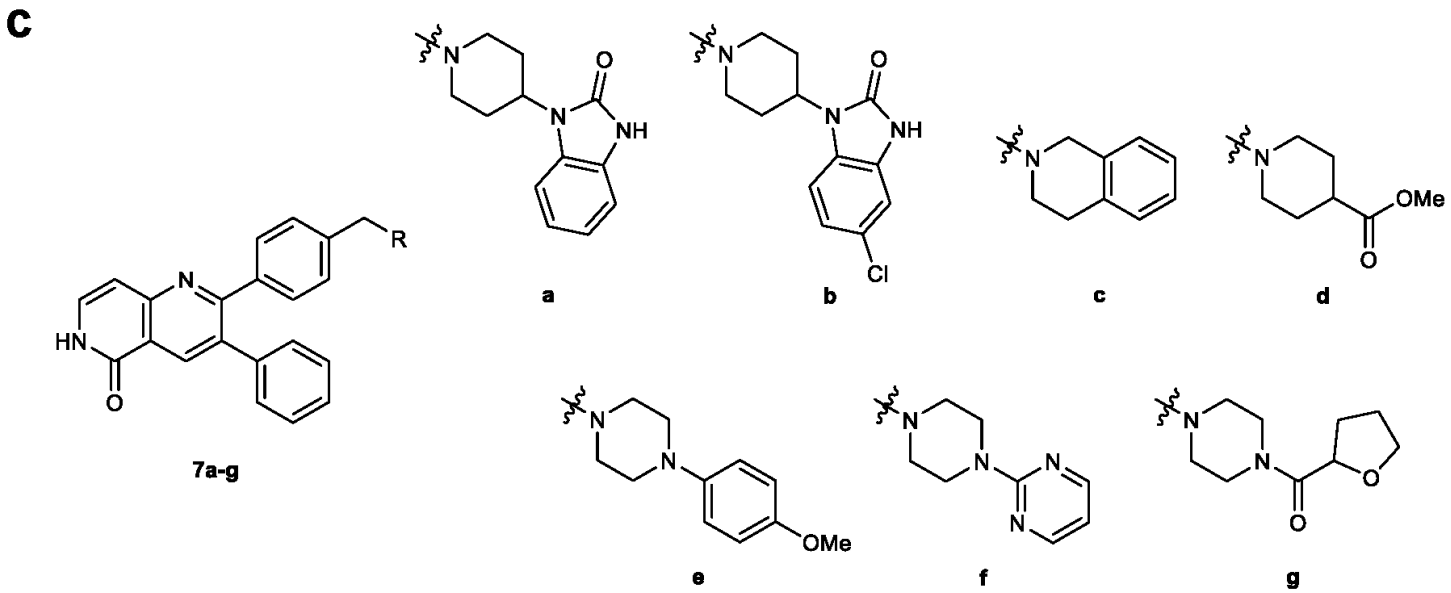

d

	IC_{50} Akt1 / µM	IC_{50} ΔPH-Akt1 / µM	GI_{50} BT474 / µM	GI_{50} H441 / µM	K_d iFLiK / µM
7a	0.033 ± 0.005	n.i.	7 ± 2	n.e.	0.41 ± 0.07
7b	0.010 ± 0.004	n.i.	3.2 ± 0.6	n.e.	0.15 ± 0.04
7c	0.9 ± 0.2	n.i.	17 ± 2	n.e.	6 ± 2
7d	0.6 ± 0.1	n.i.	18 ± 4	n.e.	0.9 ± 0.3
7e	1.4 ± 0.5	n.i.	19 ± 4	n.e.	7.2 ± 0.9
7f	0.40 ± 0.05	n.i.	13 ± 1	n.e.	1.1 ± 0.2
7g	2.1 ± 0.2	n.i.	19 ± 3	n.e.	8 ± 1
MK-2206	0.006 ± 0.002	n.i.	0.3 ± 0.1	n.e.	0.09 ± 0.01
GSK690603	0.0004 ± 0.0002	0.0007 ± 0.0004	0.7 ± 0.2	n.e.	n.r.
CCT128930	0.029 ± 0.009	0.030 ± 0.007	n.m.	n.m.	n.r.

Fang *et al.*, Figure 2

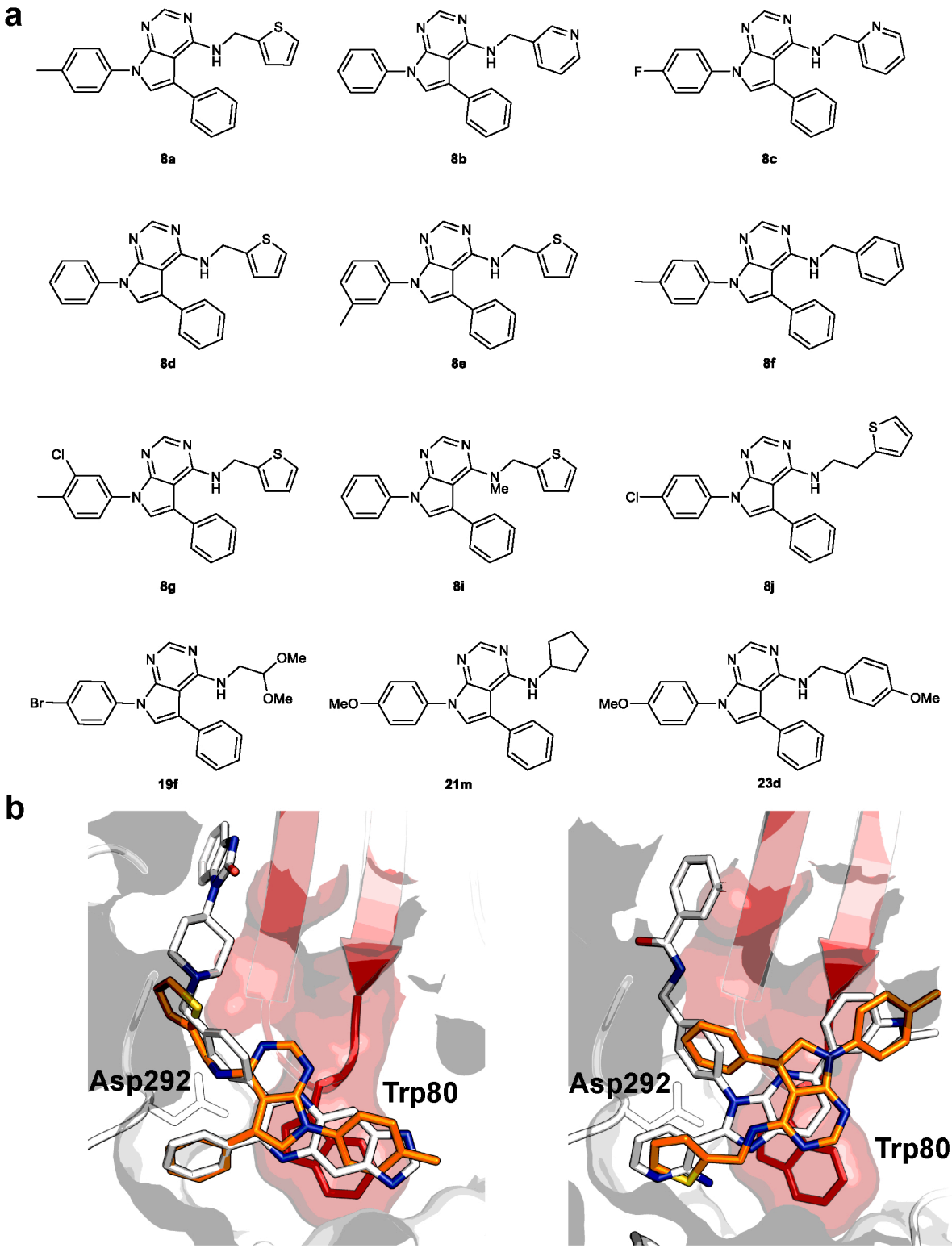

Fang *et al.*, Figure 3